Performance and Flow Calculations for a Gaseous H_2/O_2 Thruster

S. C. Kim*
Sverdrup Technology, Inc., Brook Park, Ohio 44142
and
T. J. VanOverbeke†
NASA Lewis Research Center, Cleveland, Ohio 44135

Calculations were made for the gaseous H_2/O_2 thruster designed for the space station by using the RPLUS code that employs an implicit finite-volume, lower-upper symmetric successive over-relaxation scheme to solve the Navier-Stokes equations and the species equations in a coupled manner. The combustion processes of hydrogen and oxygen are modeled by an 8-species and 18-step reaction mechanism, and the turbulence is simulated by the Baldwin-Lomax turbulence model for the thruster wall boundary layer and the modified Prandtl's mixing length model for the reacting shear layer. Results are presented for different mixture ratios and fuel film-cooling percents and compared with the experimental data. The calculated performance predictions for the thruster agree well with the experimental data, and the results demonstrate that the RPLUS code can be used for analysis of thrusters and rockets.

Nomenclature

D_{im} = effective binary diffusivity of species i in the gas mixture
e = total internal energy
F, G = inviscid fluxes
F_v, G_v = viscous fluxes
h_i = enthalpy of species i
H = source term
J = Jacobian of the transformation
k = conductivity
l = mixing length
N_s = number of species
O/F = mixture ratio (oxygen/hydrogen)
p = pressure
q = heat flux
T = temperature
t = time
u = axial velocity
$\tilde{u}_i$ = axial diffusion velocity of species i
v = radial velocity
$\tilde{v}_i$ = radial diffusion velocity of species i
$\dot{w}$ = chemical source term of species i
x, r, θ = cylindrical coordinates
Y_i = mass fraction of species i
ξ, η = generalized coordinates
μ = total viscosity, $= \mu_l + \mu_t$
ρ = density
τ = shear stress
σ = normal stress

Subscripts
cl = at centerline
c = combustor

Presented as Paper 90-2490 at the AIAA 26th Joint Propulsion Conference, Orlando, FL, July 16-18, 1990; received Oct. 9, 1990; revision received Feb. 4, 1991; accepted for publication Feb. 4, 1991.

*Senior Research Engineer, NASA Lewis Research Center Group, 2001 Aerospace Parkway, Member AIAA.
†Aerospace Engineer, MS 5-11, 21000 Brookpark Road. Member AIAA.

Introduction

THE Auxiliary Propulsion System (APS) of the manned space station provides the propulsion of various space station attitude control, orbit positioning, and docking and avoidance maneuvers. One of the candidate systems uses gaseous hydrogen and oxygen as propellants.[1,2] To design an efficient gaseous H_2/O_2 thruster with low development costs, an accurate numerical prediction of thruster performance is needed.

For the performance prediction of the rocket engine, the Joint Army, Navy, NASA, Air Force (JANNAF) Two-Dimensional Kinetics code with a boundary-layer module (TDK/BLM) has been commonly used.[3] It solves the flowfield by the Method of Characteristics with a boundary-layer correction. But the JANNAF TDK/BLM code has difficulties in solving the flow with thick boundary layers and/or reacting shear layers. Recently, efforts have been made to solve the full Navier-Stokes equations with chemical reactions. The various results for rocket engine performance predictions from Navier-Stokes codes can be found in Refs. 4-7.

In the present study, the RPLUS code, which has been developed for the National Aerospace Plane (NASP) at NASA Lewis Research Center, was selected and modified for axisymmetric flow to calculate thruster flowfields. The code was previously used to calculate two-dimensional thruster flowfields by VanOverbeke and Shuen.[7] The RPLUS code employs an implicit finite-volume, LU-SSOR scheme to solve the full Navier Stokes equations and the species equations in a coupled manner. Calculations were made for different mixture ratios and fuel film-cooling (FFC) percents and compared with experimental data.

RPLUS Code

Governing Equations

The Navier-Stokes equations and the species transport equations for axisymmetric turbulent flow can be written in the

following familiar form, where the dependent variables are mass averaged:

$$\frac{\partial Q}{\partial t}+\frac{\partial(F-F_v)}{\partial x}+\frac{1}{r}\frac{\partial[r(G-G_v)]}{\partial r}=H \tag{1}$$

$$Q=\begin{bmatrix}\rho\\ \rho u\\ \rho v\\ \rho e\\ \rho Y_i\end{bmatrix},\quad F=\begin{bmatrix}\rho u\\ \rho u^2+p\\ \rho uv\\ u(\rho e+p)\\ \rho uY_i\end{bmatrix}$$

$$F_v=\begin{bmatrix}0\\ \sigma_{xx}\\ \tau_{rx}\\ u\sigma_{xx}+v\tau_{xr}-q_x\\ -\rho\tilde{u}_iY_i\end{bmatrix},\quad G=\begin{bmatrix}\rho v\\ \rho uv\\ \rho v^2+p\\ v(\rho e+p)\\ \rho vY_i\end{bmatrix}$$

$$G_v=\begin{bmatrix}0\\ \tau_{rx}\\ \sigma_{rr}\\ v\sigma_{rr}+u\tau_{xr}-q_r\\ -\rho\tilde{v}_iY_i\end{bmatrix},\quad H=\begin{bmatrix}0\\ 0\\ -\tau_{\theta\theta}/r\\ 0\\ \dot{w}_i\end{bmatrix}$$

where

$$\sigma_{xx}=2\mu u_x-\frac{2}{3}\mu\left(u_x+v_r+\frac{v}{r}\right)$$

$$\sigma_{rr}=2\mu v_r-\frac{2}{3}\mu\left(u_x+v_r+\frac{v}{r}\right)$$

$$\tau_{xr}=\tau_{rx}=\mu(u_r+v_x)$$

$$\tau_{\theta\theta}=\frac{4}{3}\mu\frac{v}{r}-\frac{2}{3}\mu\,(u_x+v_r)-p$$

$$q_x=-kT_x+\rho\sum_{i=1}^{N_s}h_iY_i\tilde{u}_i$$

$$q_r=-kT_r+\rho\sum_{i=1}^{N_s}h_iY_i\tilde{v}_i$$

$$Y_i\tilde{u}_i=-D_{im}Y_{ix}$$

$$Y_i\tilde{v}_i=-D_{im}Y_{ir}$$

Numerical Method

In the RPLUS code, the lower-upper symmetric successive over-relaxation (LU-SSOR) scheme of Yoon and Jameson[8] is used to solve the coupled Navier-Stokes and species transport equations. The LU-SSOR scheme employs an implicit Newton iteration technique to solve the finite-volume approximation of the steady-state version of the governing equations. Even though the system of equations is formulated in a fully implicit and fully coupled manner, the LU-SSOR scheme requires only scalar diagonal inversion for the flow equations and diagonal block inversion for the species equations. This results in a fast convergence rate, and the convergence of the Newton iteration method is assured by the diagonal dominance of the coefficient matrices of the LU-SSOR scheme. Detailed description of LU-SSOR scheme can be found in Refs. 7–10.

Modifications for Axisymmetric Flow

To use the two-dimensional version of the RPLUS code with minimal modifications, the metrics were modified as follows:

$$\xi_x=rr_\eta J,\quad \xi_r=-rx_\eta J$$

$$\eta_x=-rr_\xi J,\quad \eta_r=rx_\xi J$$

$$J^{-1}=(x_\xi r_\eta-x_\eta r_\xi)r \tag{2}$$

In addition to the metrics modifications, everywhere the u_x+v_y term appears in the viscous terms of the two-dimensional code, it was replaced by u_x+v_r+v/r, and the source term, $-\tau_{\theta\theta}/r$, was included in the r-momentum equation as in the PARC code.[11]

Chemistry and Thermodynamic Transport Model

A finite-rate chemistry model of hydrogen and oxygen combustion is used in the RPLUS code, involving 8 species and an 18-step reaction mechanism. The specific heat, thermal conductivity and viscosity of each species are given as fourth-order polynomials of temperature, and the coefficients of these polynomials are valid up to a temperature of 6000 K. The specific heat of the gas mixture is obtained by concentration weighting of each species, whereas the thermal conductivity and viscosity of the gas mixture are calculated from Wilke's mixing rule. The binary mass diffusivity between two species is obtained from the Chapman-Enskog theory in conjunction with the Lennard-Jones intermolecular potential function, and the diffusion of a species in a gas mixture is approximated by Fick's law.[7,9]

Turbulence Model

The turbulence model used in the RPLUS code is that due to Baldwin and Lomax.[12] This model was used to calculate the turbulent viscosity of the thruster wall boundary layer. In addition to the Baldwin-Lomax model, the following modified Prandtl's mixing length model, in which the characteristic length scale is based on the reacting region width, was used for the reacting shear layer:

$$\mu_t=\rho l^2\left|\frac{\partial u}{\partial r}\right|=\rho C^2L_{H_2O}^2\left|\frac{\partial u}{\partial r}\right| \tag{3}$$

where C is an empirical constant ($=0.06$) and L_{H_2O} is the characteristic length scale. L_{H_2O} is obtained as follows:

1) At a given axial station, the location R_{H_2Omax} and the magnitude Y_{H_2Omax} of the maximum water mass fraction are found.

2) Between R_{H_2Omax} and the centerline, find the location R_ℓ where the mass fraction of water is $Y_{H_2Omax}-0.9(Y_{H_2Omax}-Y_{H_2O_{cl}})$.

3) Between R_{H_2Omax} and the nozzle wall, find the location R_u where the mass fraction of water is $0.1\,Y_{H_2Omax}$.

4) L_{H_2O} is the reacting shear layer width, R_u-R_ℓ.

Thruster Geometry

The thruster geometry for the present study is composed of a combustion chamber followed by a converging-diverging nozzle. Hot-fire experiments had been conducted by Aerojet General Corporation, and data are available for comparison with calculations.[13] The cutaway view of the thruster assembly and the grid for the present calculations are shown in Figs. 1 and 2. As seen from Fig. 2, the computational domain begins at the end of the cylindrical sleeve and ends at the exit of the nozzle. The total length of the computational domain is 0.273 m, and the area ratio of the nozzle is about 113. The radius of the inlet, which is located at the end of the sleeve, is 0.00856 m and the radius of the throat of the nozzle is 0.00635 m.

Figure 3 shows the inlet geometry and the inflow conditions at the inlet. As seen from this figure, the core flow consists of

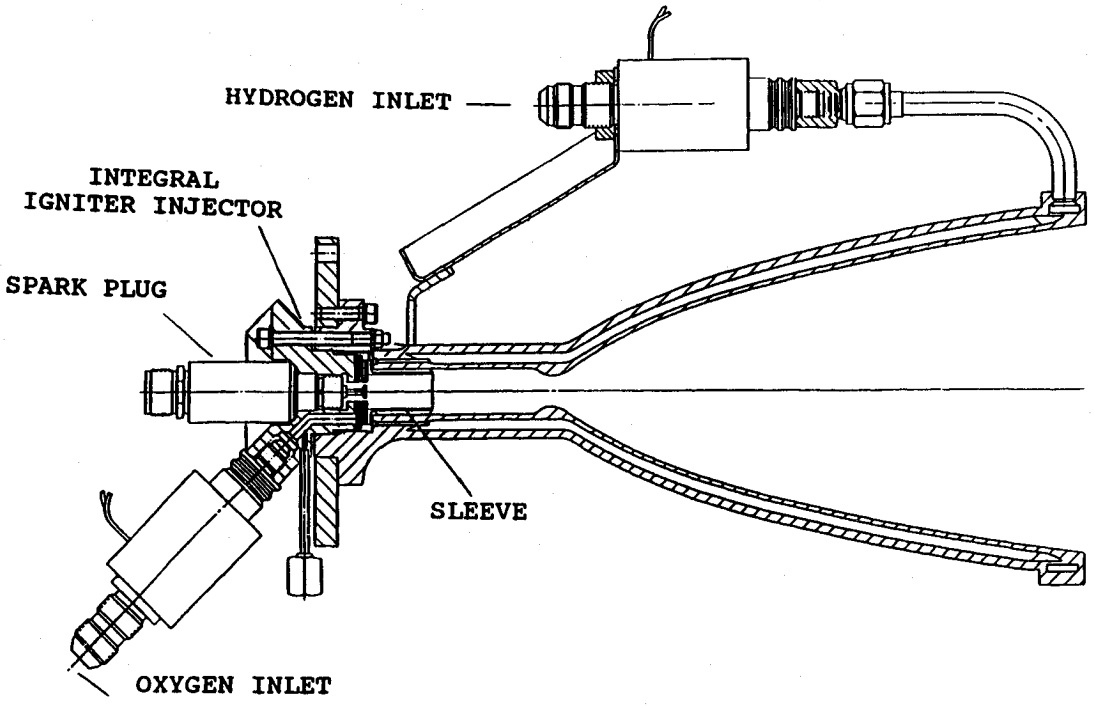

Fig. 1 Cutaway view of the thruster assembly.

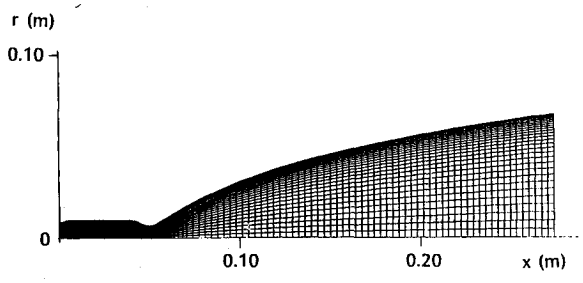

Fig. 2 Computational grid.

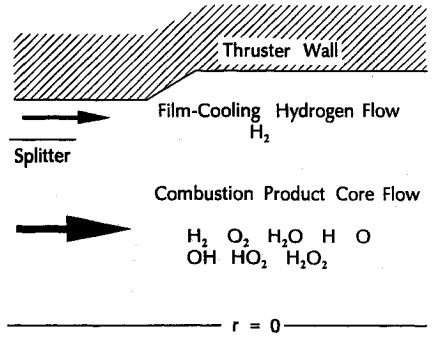

Fig. 3 Inlet conditions.

Table 1 Inflow conditions

	Case 1	Case 2
O/F	3.89	6.67
FFC, %	51.7	58.5
P_c, atm	5.1	5.1
Core flow		
O/F	8	16
T, K	3300	3073
Mass fraction		
H_2	0.019	0.002
O_2	0.100	0.433
H	0.004	0.001
O	0.029	0.026
OH	0.123	0.084
H_2O	0.725	0.454
Hydrogen flow		
T, K	522	522
Mass fraction		
H_2	1.0	1.0

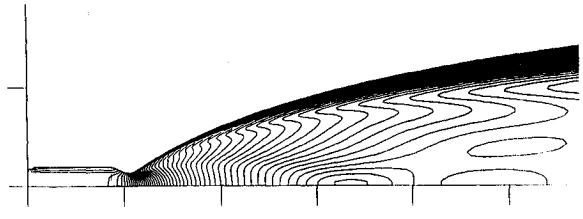

Fig. 4 Mach number contours ($O/F = 3.89$ and FFC = 51.7%).

combustion products. In the present study, it was assumed that the reactions inside the combustor core have been completed before the end of the sleeve and the combustion products are in chemical equilibrium. The hydrogen fuel is used to regeneratively cool the thrust chamber and collected in an annular manifold that feeds two sets of radial flow passages. One set of radial passages supplies some of the hydrogen to the injector and the other set directs the remaining hydrogen into slotted passages within the cylindrical sleeve to inject as film-cooling hydrogen along the thruster wall.

The combustion product flow and the hydrogen flow are separated by a cylindrical sleeve with milled slots for film-cooling hydrogen, but for simplicity it was assumed in the present study that the two flows are separated by a zero thickness splitter and the slotted injector passages for the film-cooling hydrogen are approximated by an annulus whose area matches the total slot area.

Inflow Conditions

The combustor pressure and mixture ratio of the core flow were obtained from experiments. For a given combustor pressure and mixture ratio, the mass fractions of the eight species were obtained by running the CET85 computer program of Gordon and McBride[14] that calculates the chemical equilibrium compositions for a given pressure and mixture ratio.

GEO. It also increases with inclination due to higher relative velocities between the satellite and the objects in GEO. For example, a decrease of two orders of magnitude is apparent for a spacecraft in an orbit with an inclination of 1 deg at ± 100 km above or below GEO.

IV. Disposal Options

Some of the satellites launched into the geosynchronous orbit have been removed at the end of life to either higher or lower altitudes. The primary benefits for removing old spacecraft from the geosynchronous orbit are 1) freeing of desirable longitudinal positions for replacement spacecraft to avoid interference from old spacecraft and 2) reduction of collision damage potential for other spacecraft.

The removal of inactive satellites has evidently become a practice at Intelsat and the European Space Agency (ESA). The first case of end-of-life removal occurred in May 1977, when three Intelsat 3 satellites F2, F3, and F4 were moved to disposal orbits at 3580-, 3700-, and 400-km altitudes beyond the altitude of the geosynchronous orbit.[6] The ATS 6, Raduga 5, Anik 1, SMS 1, SMS 2, and Intelsat 4 F2 and F4 were removed later to disposal orbits at 3580-, 3700-, and 4000-km altitudes beyond the altitude of the geosynchronous orbit.[6] The ATS 6, Raduga 5, Anik 1, SMS 1, SMS 2, and Intelsat 4 F2 and F4 were removed later to disposal orbits. Similarly, in January 1984, GEOS 2 was placed 269 km above GEO by ESA using 2 kg of propellant in three impulses.

Similar requirements are placed on future spacecraft by the U.S. Navy UHF Follow-On, DSCS-III, and so forth, which require removal of satellites to supersynchronous orbits by at least 370 km from GEO. Also, AUSSAT, the Australian Agency, requires removal capability of up to 1110 km above GEO at the end of life.

The practice of removing satellites from GEO is not without some risk and cost to the spacecraft operator. The risk is the probability of failure during the maneuver, which may result in an orbit with higher relative velocities or even a collisional breakup. The cost is the slightly reduced life and the potential loss of the satellite as a spare or a decoy. (The latter may sometimes be of benefit to military spacecraft.)

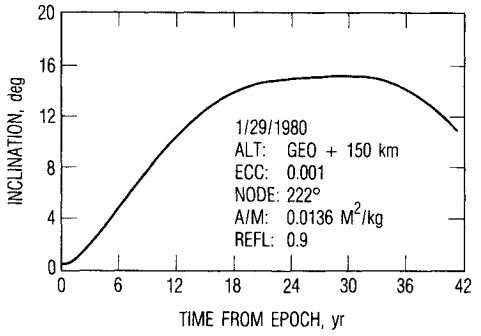

Fig. 11 Inclination drift in supersynchronous orbit.

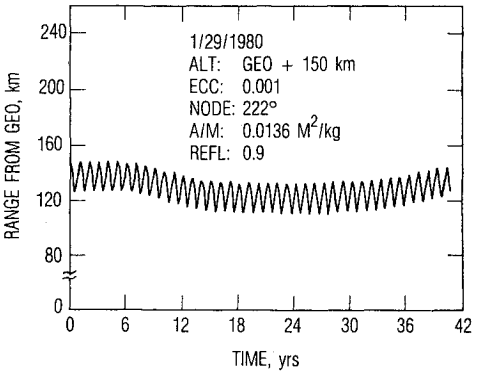

Fig. 12 Perigee drift in supersynchronous orbit.

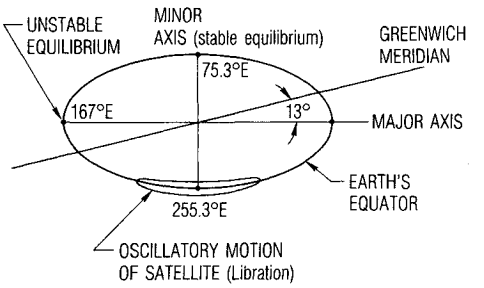

Fig. 13 Geopotential stable points.

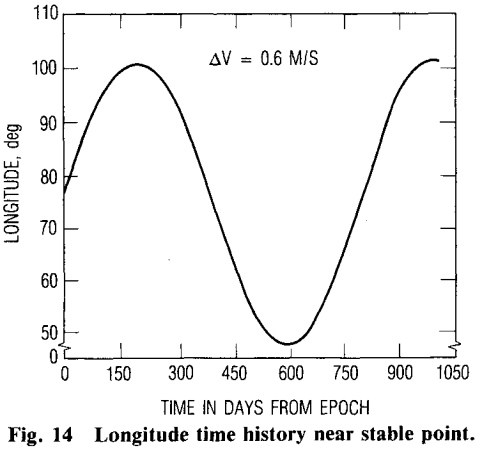

Fig. 14 Longitude time history near stable point.

In view of this, decisions concerning removal of a spacecraft at the end of life should be made only after careful analysis of all factors. To minimize the explosion hazard from fuel decomposition, a burn to depletion of propellants should also be considered.

A. Supersynchronous Orbit Disposal

The potential for reduction of the probability of collision is illustrated in Fig. 10, which shows that a two- or three-order-of-magnitude decrease in the collision hazard results by placing a spacecraft about 300 km above the geosynchronous orbit. The velocity impulse for such a maneuver is only 10.8 m/s requiring, for example, only 5 to 10 kg of propellant for a typical spacecraft. This translates to a month or two of life reduction and can be accomplished by a two-impulse maneuver.

The technique of initially deploying satellites to a supersynchronous orbit can also be used to ensure that the apogee-injection stage remains above geosynchronous. This procedure is attractive in that it effectively removes the threat posed by the apogee-injection stage to objects in the geosynchronous corridor.

The long-term stability of supersynchronous orbits has been examined numerically using program ELEMENT[7] and found to be satisfactory. For example, the first order, nearly resonant perturbation for circular orbits displaced in an altitude ± 150 km from a typical synchronous, nearly equatorial orbit results in the maximum radial excursion on the order of only ± 2.31 km almost entirely due to the lowest order tesseral harmonic $J_{2,2}$.

The effects on the sun/moon perturbation, however, will cause an orbital inclination growth from zero to nearly 15 deg in 27.4 years, as illustrated in Fig. 11. The in-plane motion, on the other hand, is caused mostly by solar radiation pressure. For example, for an object with an area-to-mass ratio of 0.014 m^2/kg and a coefficient of reflection of 0.9, the maximum cyclical perigee altitude variation is only about 24 km/yr. A longer-term perigee variation of about 20 km is also apparent in Fig. 12, which illustrates the perigee drift due to solar radiation pressure. For a detailed description of the general inclination history, see Ref. 8.

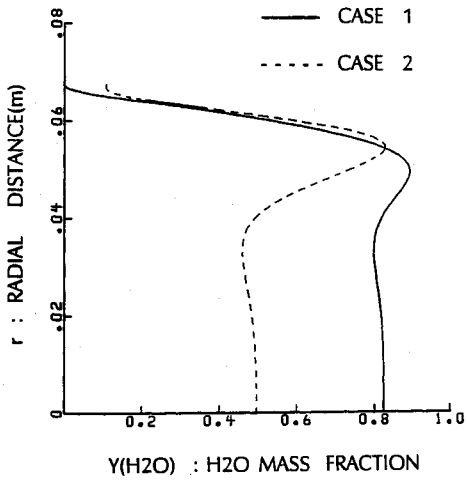

Fig. 12 H_2O mass fraction vs radial distance at the exit of the nozzle.

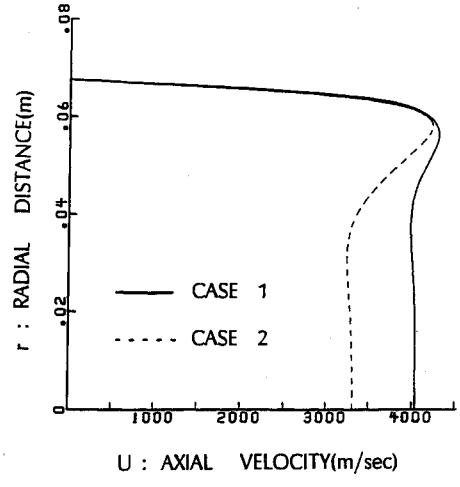

Fig. 13 Axial velocity vs radial distance at the exit of the nozzle.

the cold film-cooling hydrogen flow, the Mach number and temperature contours are quite different from those for nozzles without film-cooling hydrogen flows.[4,15] The H_2O contours are shown in Fig. 6. High values of H_2O mass fraction are observed at the reacting shear layer between the core flow and the hydrogen flow. The results for case 2, which corresponds to oxygen-rich combustion in the combustor, are presented as Mach number, temperature, and H_2O mass fraction contours in Figs. 7-9. As seen from these figures, the contours are similar to those for case 1.

Figures 10-13 show the Mach number, static temperature, H_2O mass fraction and axial velocity profiles at the exit of the nozzle for both cases 1 and 2. As seen from Fig. 10, the maximum Mach number is observed near the reacting shear layer for both cases, and the Mach number profile for case 2 is nearly the same as that for case 1 except inside the boundary layer and near the reacting shear layer where the Mach number for case 2 is smaller than that for case 1. Due to the chemical reactions between the oxygen in the core flow and the hydrogen in the film-cooling flow, the temperature inside the boundary layer and near the reacting shear layer for case 2, which corresponds to the oxygen-rich core flow, is higher than that for case 1, which corresponds to stoichiometric core flow, even though the temperature of the core flow at the inlet for case 2 is lower than that for case 1 as shown in Fig. 11. The profiles of H_2O mass fraction for both cases in Fig. 12 clearly show the reacting shear layers. The H_2O mass fraction for case 2 is higher than that for case 1 at the nozzle wall because of the oxygen-rich core flow for case 2. The axial velocity for case 1 is larger than that for case 2 as shown in Fig. 13. Because a hydrogen-rich flow has a high exhaust velocity due to its low

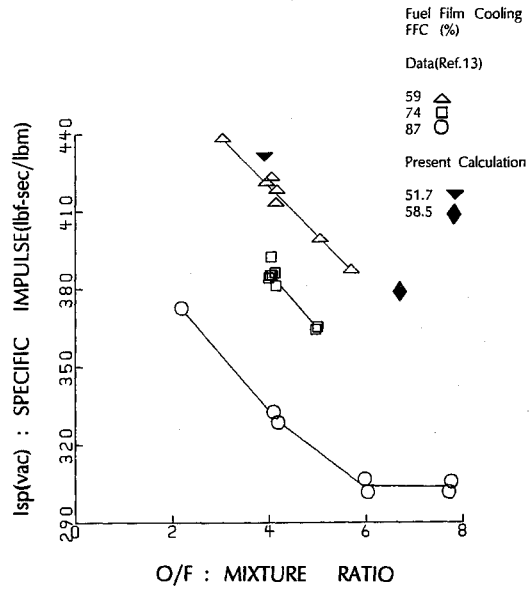

Fig. 14 Specific impulse vs mixture ratio.

molecular weight, the largest axial velocity was observed near the edge of the nozzle wall boundary layer where the values of H_2 mass fraction are high.

The calculated specific impulses are shown in Fig. 14 and compared with the experimental data for various mixture ratios and FFC percents. As seen from this figure, the current results show the decrease of specific impulse with increasing mixture ratio and agree well with the experimental data.

Conclusion

The gaseous H_2/O_2 thruster was studied numerically using the axisymmetric version of the RPLUS code that employs an implicit finite-volume, LU-SSOR scheme to solve the Navier-Stokes equations and the species equations. The combustion processes of hydrogen and oxygen are modeled by an 8-species and 18-step finite-rate reaction mechanism, and the turbulence was simulated by the Baldwin-Lomax turbulence model for the thruster wall boundary layer and the modified Prandtl's mixing length model for the reacting shear layer. Both the case for an overall mixture ratio of 3.89 and FFC of 51.7% and the case for an overall mixture ratio of 6.67 and FFC of 58.5% were calculated. Results were presented as Mach number, temperature, and H_2O mass fraction contours and profiles and the calculated specific impulses were compared with the experimental data. The calculated specific impulses of the thruster agree well with the measured values. The present study demonstrates that the RPLUS code predicts the performance of the thruster accurately, and it can be used for analysis of chemical rockets.

Acknowledgments

The work of the first author was supported by NASA Lewis Research Center under Contract NAS3-25266 with Raymond E. Gaugler as the monitor. The authors would like to thank J.-S. Shuen of Sverdrup Technology, Inc., for supplying the two-dimensional version of the code and for help during the course of the present study. This work was performed using the computational resources of the National Aerodynamic Simulation Facility.

References

[1]Jones, R. E., Morren, W. E., Sovey, J. S., and Tacina, R. R., "Space Station Propulsion," NASA TM-100216, Dec. 1987.

[2]Richter, G. P., and Price, H. G., "Proven, Long-Life Hydrogen/Oxygen Thrust Chambers for Space Station Propulsion," NASA TM-88822, Aug. 1986.

[3]Nickerson, G. R., Coates, D. E., and Bartz, J. L., "Engineering

Programming and Users Manual; Two-Dimensional Kinetic Reference Computer Program," NASA CR-152999, Dec. 1973.

[4]Dang, A. L., Kehtarnavaz, H., and Coats, D. E., "The Use of Richardson Extrapolation in PNS Solutions of Nozzle Flow," AIAA Paper 89-2895, July 1989.

[5]Sinha, N., York, B. J., Ong, C. C., and Dash, S. M., "3D Navier-Stokes Analysis of High Speed Propulsive Flowfields Using Parch Code," AIAA Paper 89-2796, July 1989.

[6]Trinch, H. P., and Gross, K. W., "Interaction of External Conditional with the Internal Flowfield in Liquid Rocket Engine (A Computational Study)," AIAA Paper 89-2894, July 1989.

[7]VanOverbeke, T. J., and Shuen, J.-S., "A Numerical Study of Chemically Reacting Flow in Nozzle," NASA TM-102135, July 1989.

[8]Yoon, S., and Jameson, A., "A LU-SSOR Scheme for the Euler and Navier-Stokes Equations," AIAA Paper 87-0600, Jan. 1987.

[9]Shuen, J.-S., and Yoon, S., "Numerical Study of Chemically Reacting Flows Using a LU-SSOR Scheme," *AIAA Journal*, Vol. 27, No. 12, Dec. 1989, pp. 1752–1760.

[10]Yu, S. T., McBride, B. J., Hsieh, K. C., and Shuen, J.-S., "Numerical Simulation of Hypersonic Inlet Flows with Equilibrium or Finite Rate Chemistry," AIAA Paper 88-0273, Jan. 1988.

[11]Cooper, G. K., "The PARC Code: Theory and Usage," Arnold Engineering Development Center, Arnold AFB, TN, AEDC-TR-87-24, Oct. 1988.

[12]Baldwin, B. S., and Lomax, H., "Thin Layer Approximation and Algebraic Model for Separated Turbulent Flows," AIAA Paper 78-0257, Jan. 1978.

[13]Robinson, P. J., "Space Station Auxiliary Propulsion System," NASA CR-185296, July 1990.

[14]Gordon, S., and McBride, B. J., "Computer Program for Calculation of Complex Chemical Equilibrium Compositions, Rocket Performance, Incident and Reflected Shocks, and Chapman-Jouguet Detonations," NASA SP-273, March 1976.

[15]Benton, J., and Perkins, J., "Limitations of Method of Characteristics When Applied to Axisymmetric Hypersonic Nozzle Design," AIAA Paper 90-0192, Jan. 1990.

James A. Martin
Associate Editor